



Experimental and Numerical Study of HSLA Steel Fatigue and Pitting Corrosion Behavior

Arwa Toumi · Chokri Boubahri · Jalel Briki

Submitted: 31 October 2022 / Accepted: 16 November 2022 / Published online: 6 December 2022
© ASM International 2022

Abstract This paper presents an experimental and numerical study of the fatigue-corrosion behavior of the high strength low alloy steel known as HSLA steel in marine environment. Based on a case study of steel removed from of hull ship after about 1300 h of service in seawater, microstructural fatigue-corrosion indicators are detected such as micro-cracks, micro-pits, and beach marks. In addition, the mechanical properties decreased dramatically. Pitting corrosion acts as the main phenomena leading to the metal deterioration. This is confirmed through electromechanical calculation and potentiodynamic curves. Since, the environment is harsh and out of our control, a numerical study of the effect of pitting and the coupling between fatigue and pitting corrosion is held. The results show that the geometry of corrosion defect is responsible for the propagation of the pit and can lead to the crack formation. von Mises stress propagation is controlled too by the corrosion potential distribution.

Keywords Metallurgy · Corrosion-fatigue · Case study · Numerical modeling · Corrosion potential distribution

Introduction

Corrosion is widely known to be a complex phenomenon depending on different parameters that include environment conditions, surface, and manufacturing conditions of the considered metal [1]. For the use of HSLA steel in naval construction, the situation is more serious because of the coupling between electrochemical and mechanical factors inducing the degradation of the metal [2, 3]. The effect of corrosion on fatigue life has been widely studied [4–6]. Indeed, it is estimated that the presence of corrosion pits or generally heterogeneities in the structure considerably reduces the fatigue life of the material [7]. These pits are in the form of geometric defects which subsequently facilitate the initiation of cracks by the effect of local concentration of stresses. Thus, in the work of the referred researchers [8], they observed that the fatigue life decreases sharply when the pre-corrosion time increases and then saturates for long immersion times. In other research conducted on stainless metals, it is found that the reduction in fatigue life with pre-corrosion time is greater for low loading levels, hence for long lifespans [9]. For the case of HSLA steels according to [10], it has been shown that the number of fatigue cycles until failure has been radically affected by exposure to corrosion. In addition, the mode of failure has been affected; indeed, the uncorroded samples showed axisymmetric ductile failure modes. The failure mode of the corroded specimens was not axisymmetric and also included a low cycle fatigue brittle failure mode. In research conducted on E690 steel of the HSLA family, it is found that the base metal and the simulated HAZ (heat affected zones) of the steel are susceptible to corrosion fatigue cracking in a marine atmosphere containing SO₂ (sulfur dioxide), and the failure mode becomes brittle

A. Toumi (✉) · C. Boubahri · J. Briki
Search Unit Energy and Environment, National School of Engineering of Tunis, Tunis Le Belvédère 1002, Tunisia
e-mail: arwatoumi123@gmail.com

A. Toumi · C. Boubahri · J. Briki
Naval Academy, Menzel Bourguiba, Tunisia

intergranular [11]. Another research comparing the two steel grades HSLA-80 and HSLA-100 shows that the behavior in air is indistinguishable, regardless of differences in microstructures [12]. However, in a corrosive atmosphere, HSLA-100 steel showed slightly lower resistance to fatigue crack growth than HSLA-80 steel. The poor corrosion fatigue crack propagation resistance of HSLA-100 steel can be attributed to the rapid film formation and failure resulting from its high polarization ability and susceptibility to planar failure mode. The present work deals with two main issues, the first is the investigation on the main cause of degradation of the metal through a case study, and the second is the behavior of the considered metal coupling the two physics which are mechanics and electrochemistry, and it is held through numerical studies.

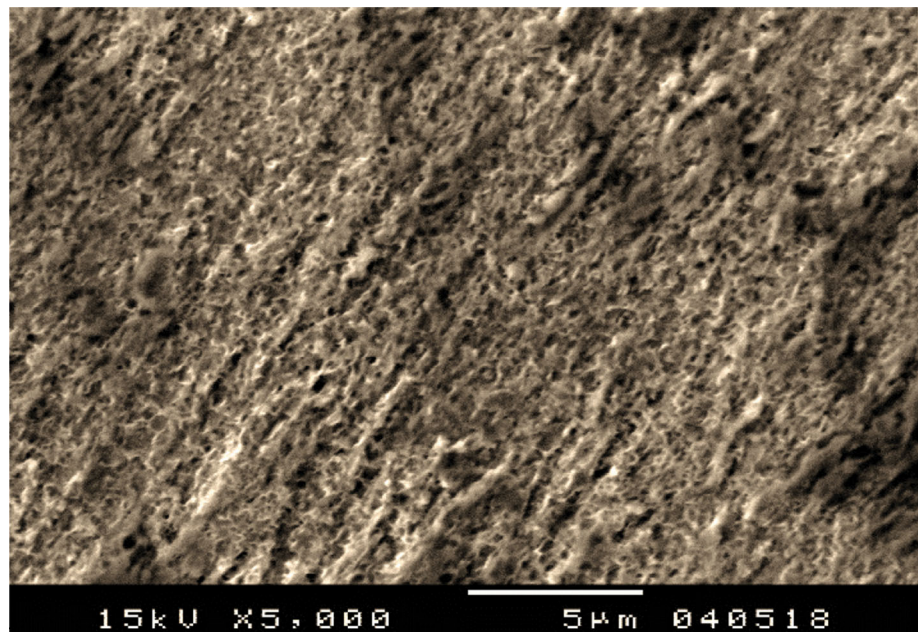
Table 1 Chemical composition

Elements	C	Si	Mn	P	S	Cr	Ni	Cu	Mo
wt.%	0.15	0.18	0.87	0.029	0.004	0.02	0.01	0.013	0.001

Table 2 Mechanical properties

Mechanical properties	Tensile strength (MPa)	Yield strength (MPa)	Elongation %	Hardness HB
	328	467	28	475

Fig. 1 Microstructure of HSLA steel grade NV EH 32 (ferritic structure with pearlite)



Experimental

Materials and Methods

In this section, materials and methods are presented. The high strength low alloy steel grade NV EH 32 is used in the study. The chemical and mechanical properties are given in Tables 1 and 2. The microstructure of the base metal is ferritic as shown in Fig. 1.

Fatigue Behavior in Real Conditions

TO study fatigue behavior of the considered HSLA steel, an experimental investigation in real conditions of service is held. In fact, since it is used in the construction of ship hull, the steel cannot be easily simulated in laboratory on a fatigue test machine. This is due mainly to the non-uniform cycles and stress conditions. The samples are taken from a 27-m length ship served for about 37 years as shown in Fig. 2. After sandblasting to remove the layers of anti-fouling painting, the steel is cleaned with SiC paper then polished and etched with nital solution to undergo microstructure investigation.

A monotonic tensile test is carried out on a universal testing ZwickRoell machine. The results show a decrease in both tensile and yield strength from, respectively, 328 and 467 to 290,388 MPa. Hence, the elastoplastic behavior changed due to the change in the metal structure with the formation of more discontinuities in the core of the steel. As shown in Fig. 3, the images obtained from scanning electron microscope SEM reveal the presence of multiple of indicators of fatigue phenomena. As is clear in Fig. 3a,



Fig. 2 (a) Removal of samples from damaged ship hull (b) pitting corrosion on the surface of the steel

the presence of micro-cracks is obvious with the direction parallel of that cold-rolling (that underwent the steel during the manufacturing process) and which can be caused by the residual stress. The arrangement of beach marks is obvious and indicates the irregular cycling mode.

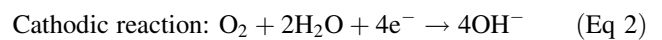
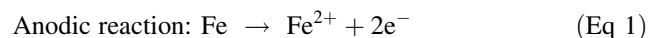
The second type of cracks is shown in Fig. 3b. The micro-cracks are initiated from the bottom of the corrosion pit. In Fig. 3c, the presence of beach marks and striation is illustrated. Those latter are a proof of fatigue happening on the metal. With some further failure analysis, we can determine the condition of loading and where the crack started.

Electrochemical Investigations

Electrochemical tests were carried out on the steel. The setup included a potentiostat connected to a computer for controlling the tests and acquiring the data, and an electrochemical cell with three electrodes: a reference electrode with saturated calomel (ECS) in chloride potassium KCl ($E = 241 \text{ mV/ENH}$) to simulate the sea water environment, a counter electrode (CE) consisting of a platinum grid and a sample of NV EH32 steel taken as the working electrode (WE). The results shown in Fig. 4 indicate that for the base metal, the anodic passivation behavior is typical where there is a passivation plateau. At this stage, the material tries to resist corrosion except that at the value ($E_p = 0.6 \text{ V}$), we notice a small return which indicates the beginning of a corrosion phenomenon by pitting and which indicates what is called the pitting potential.

Numerical Study

It is found after the case study held in the previous section that it consists of fatigue corrosion occurring on the steel. The relation between the formation of pits and micro-cracks is still not well explained. To understand the behavior of pits and micro-cracks in the HSLA steel in corrosive atmosphere a numerical study using COMSOL Multiphysics [13] is held in this section. The model used in this section uses the coupling of two physics, while it is a case of simultaneous mechanical and electrochemical behavior [14]. A two-dimension model of the steel plate is considered with very small dimensions as mentioned in Fig. 5. For the electrolyte section, we simulated the marine environment with 3.5% sodium chloride solution. We supposed that it is a reduction of oxygen that happens in the electrolyte, while the environment is aerated as explained in Eqs 1 and 2.



The electrochemical parameters are obtained from the potentiodynamic curves, and the cathodic and anodic reactions are modeled using the Tafel equations

$$\varphi_{a,eq} = \varphi_{a,eq}^0 + \frac{0.0592}{2} \text{Log} [\text{Fe}^{2+}]$$

$$\varphi_{c,eq} = \varphi_{c,eq}^0 + \frac{0.0592}{8} \text{Log} [\text{O}^{2-}]$$

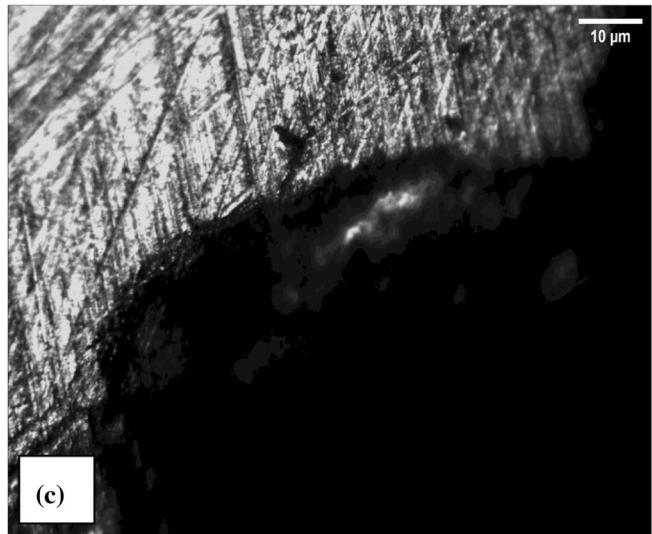
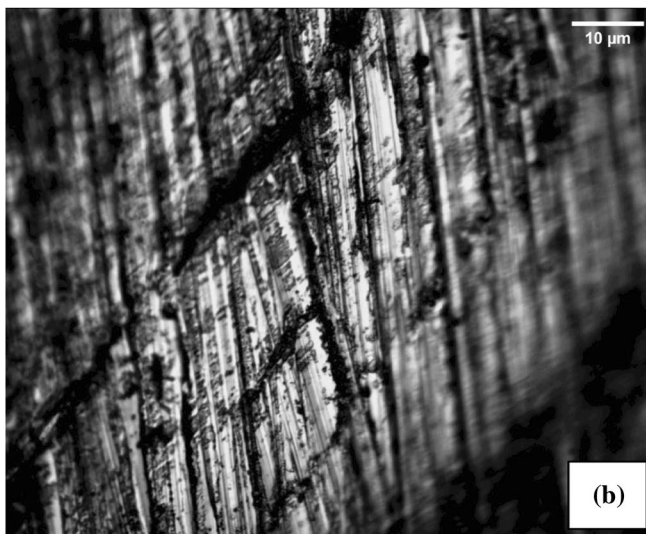
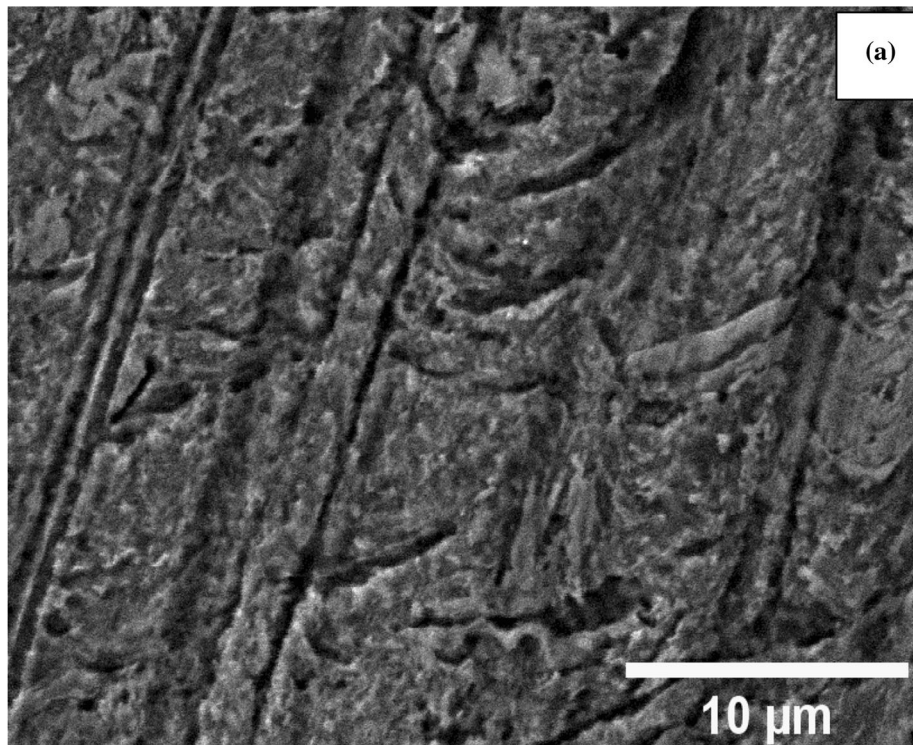


Fig. 3 Images obtained from scanning electron microscope SEM reveal the presence of multiple of indicators of fatigue phenomena: (a) beach marks and micro-cracks (b) propagation of cracks (c) initiating of cracks from pits

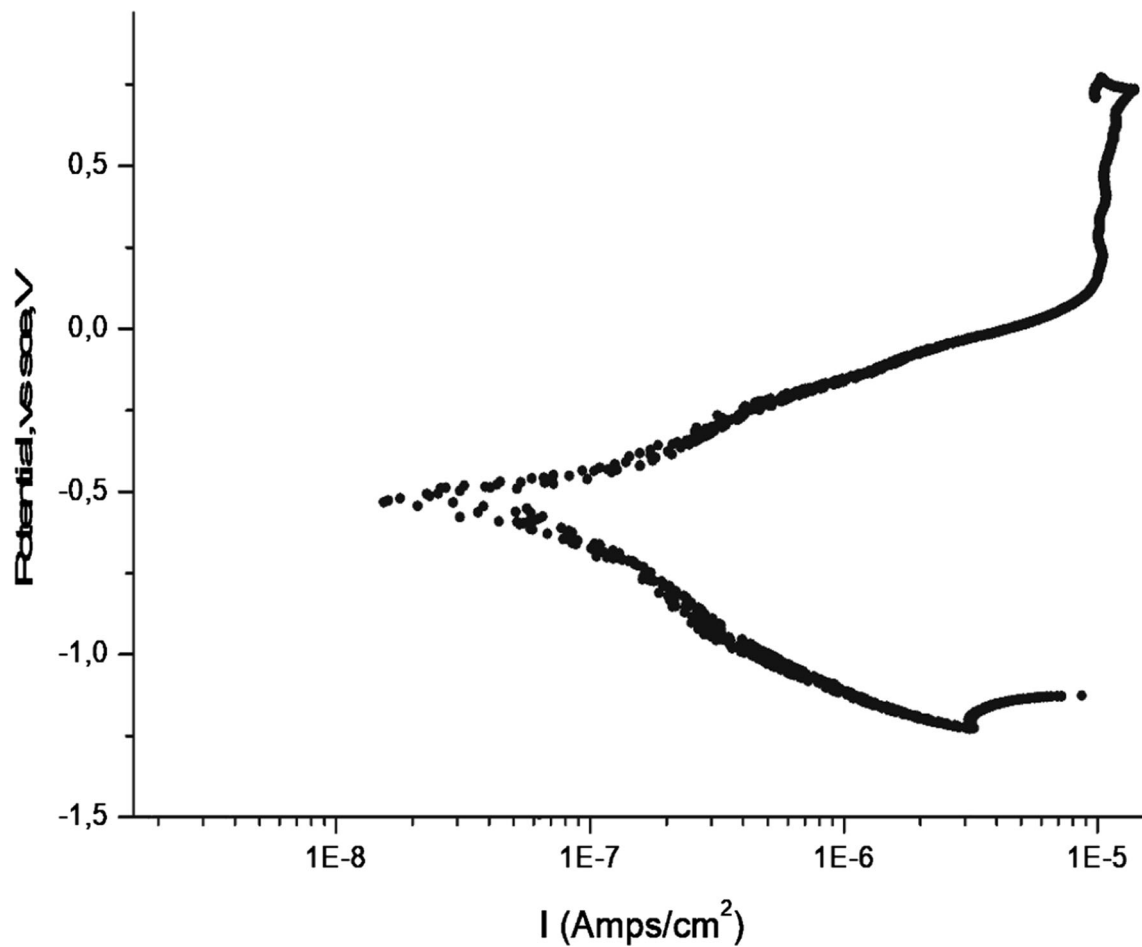


Fig. 4 Potentiodynamic curve of HSLA NVEH32 steel in 3.5% NaCl solution

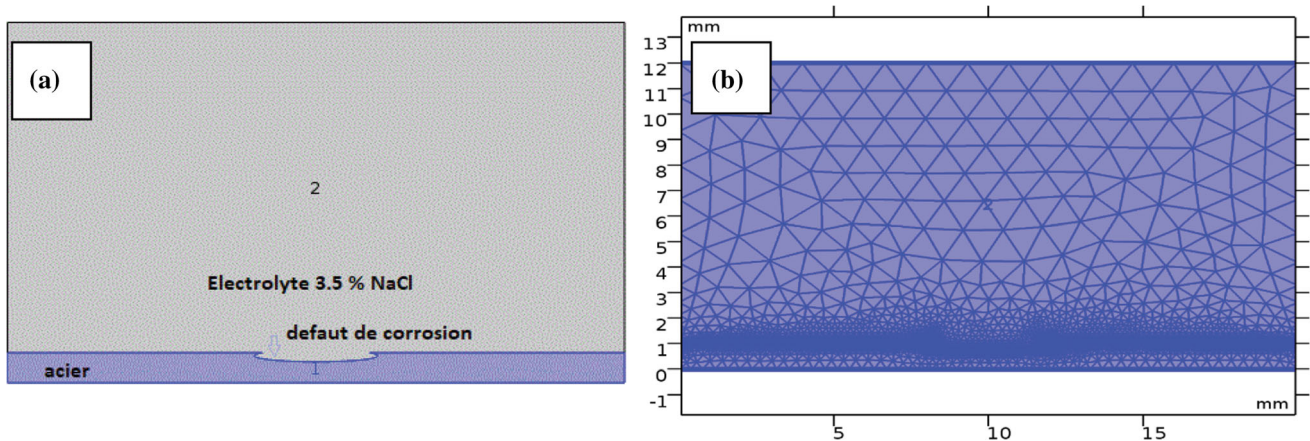


Fig. 5 (a) The 2D model of the numerical study of mechano-electrochemical behavior of HSLA steel. (b) Meshing of the model with refining meshing of the contact surface between electrode and electrolyte

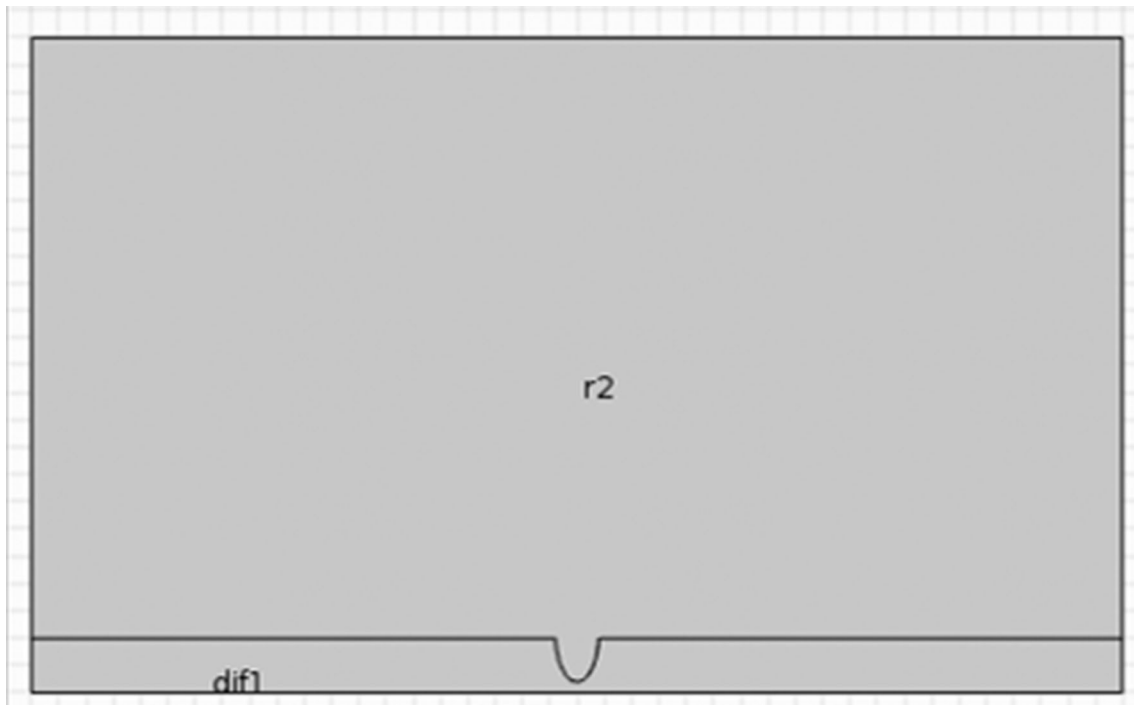


Fig. 6 The 2D model of the numerical study of mechano-electrochemical behavior of HSLA steel with narrow and deep defect

where subscripts a and c refer to anodic and cathodic reactions, and φ_{eq} is equilibrium electrode potential. The equilibrium potentials of the oxidation of iron and oxygen evolution are determined by Nernst equations.

Results and Discussion

First, we notice a reduction in the potential near the upper contours of the pit when the behavior is still elastic, and the stresses are distributed in a way equivalent to the case of the absence of corrosive agents. This zone, given its slightly pointed geometry, is more vulnerable to a reduction of the metal since it can besiege the chemical elements responsible for corrosion (mainly hydrogen and oxygen) and therefore a relationship cannot be established between the influence of stresses on the distribution of corrosion

potential and vice versa. However, we note that when we increase the displacement values (22 and 27%), approaching the plastic limits of the metal, the von Mises stress values increase at the bottom of the pit, we also see a remarkable decrease in the corrosion potential, which indicates that this area has become more vulnerable to the development of the corrosion phenomenon. Indeed, the mechanical stress favors the embrittlement of this zone which will subsequently favor the sequence of the rupture of the passive film and the reduction of the metal.

It has been shown that the shape of the pit is also involved in the kinetics of electrochemical behavior [15–17]. In the first case, we used a wide and flat type of corrosion defect with irregular sides. In the second and third case illustrated in Fig. 6, a narrow and deep type of pits was used. We noticed, as well as the stress concentration of von Mises is localized in bottom of the pits, and

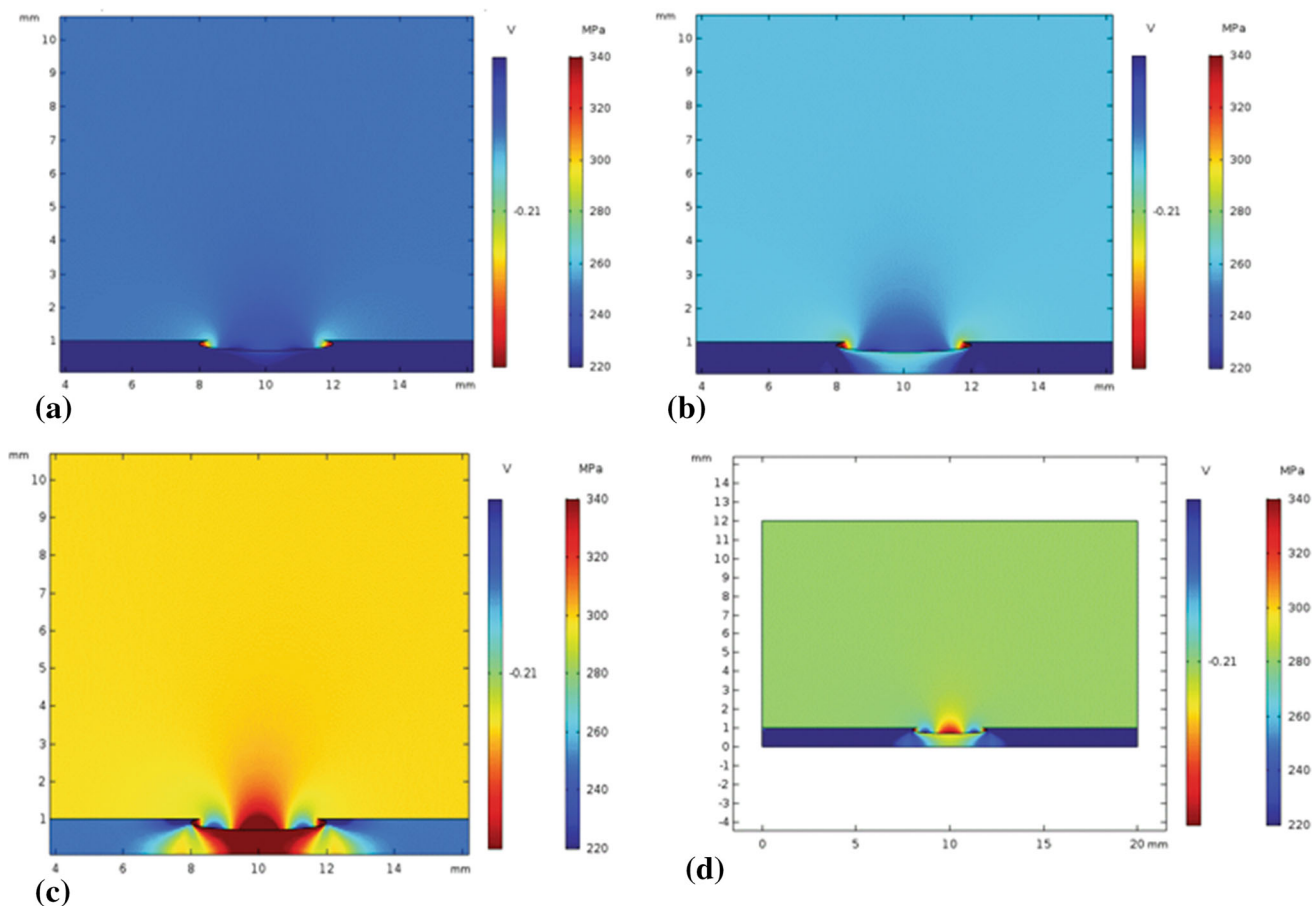


Fig. 7 Distribution of the corrosion potential in the electrolyte and the distribution of the Von stresses placed at the level of the corrosion defect for the following imposed displacement values (a) 17%, (b) 20%, (c) 22% and (d) 27%

they are propagated in depth of the metal when we increase the value of imposed displacement. The corrosion potential has decreased considerably, and its value is lower than that where the defect was flat and wide (difference of 0.02 V) Fig. 7.

We notice that by increasing the imposed displacement two types of behavior can happen. First, the stress which is concentrated in the bottom region of the pit can lead to the formation of crack when an energetic instability is reached. Second, it can lead to the formation of pits around the corrosion defect as shown in Fig. 8d, this region is weakened and the von Mises stress is increasing which explains the possibility of formation of new pits.

The third simulation was carried out on a model of a plate with corrosion defect that contains a micro-crack in the bottom, Fig. 9. When there is an electrochemical exchange of reduction at the level of the pit associated with an increase in stresses, the latter can propagate in depth to lead to a hole, or when there is an energy imbalance resulting from the concentration of the stresses at this location, there may be cracking for this second case. It is shown by the simulation's results that the micro-crack is acting as a new pit and the behavior is similar of that when the pit was considered narrow and deep. In addition, we can notice that the upper sides of the pit are weakened with increasing the imposed displacement which can lead to the

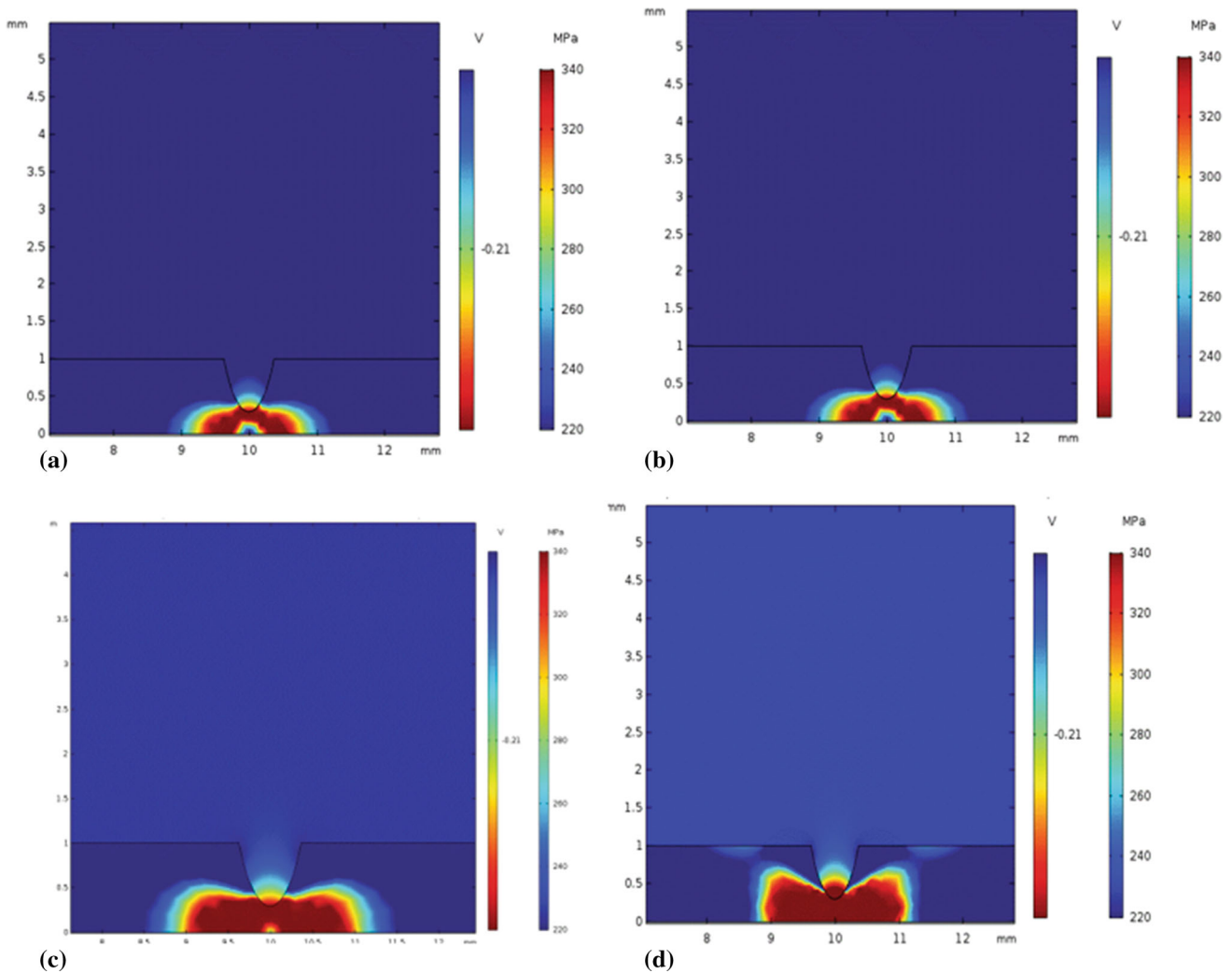


Fig. 8 Distribution of the corrosion potential in the electrolyte and the distribution of Von stresses leveled at the narrow and deep type corrosion defect for the following imposed displacement values (a) 17%, (b) 20%, (c) 22% and (d) 27%

propagation of the reduction of metal at this region if the corrosion potential is reached (the propagation of pit in depth is seen only in the case of imposed displacement 27%) or the propagation of the micro-crack.

Conclusion

In this paper, the electromechanical behavior of HSLA grade NV EH 32 steel is experimentally and numerically investigated. In fact, this work came up with interesting non-in-laboratory and numerical results cited as below:

- It was found that in real condition of service of steel used in hull constructions, an inevitable case of fatigue

corrosion will occur. This is highlighted by the formation of beach marks indicating the irregular cycling modes.

- Pitting corrosion is mainly the dominant form of corrosion occurring, and a relation between micro-cracks and pits evolution was showed through microscopy.
- A numerical study is set to understand this latter relation based on coupling physics through Guttman theory.
- The geometry of pits and its shape are involved in the mode of propagation and evolution of the latter when it is mechanically stressed. So, the deeper and narrower the shape, the more the corrosion potential decreases, which favors the reduction of the metal either by

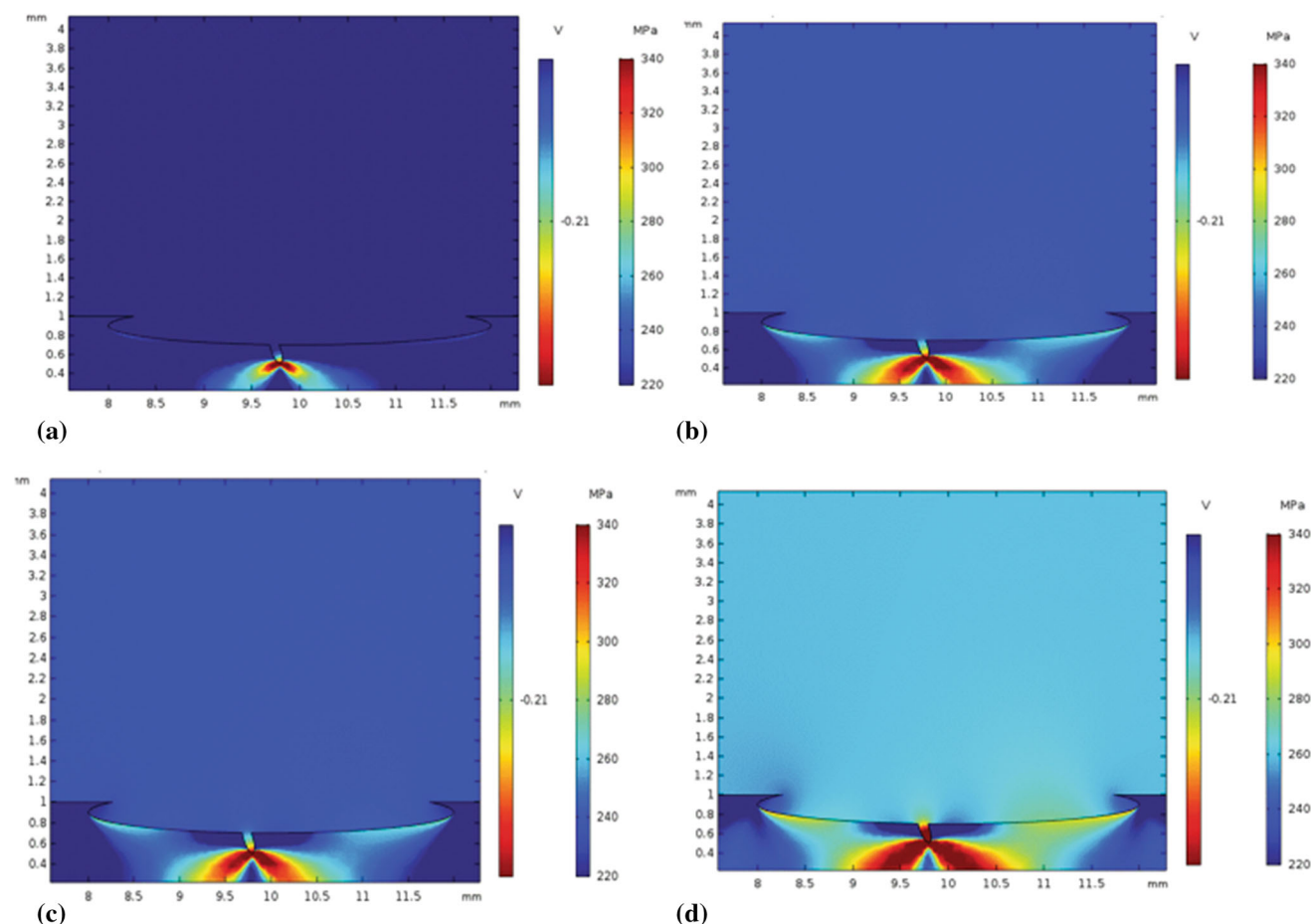


Fig. 9 Distribution of the corrosion potential in the electrolyte and the distribution of the Von stresses placed at the level of the narrow and deep corrosion defect for the following imposed displacement values (a) 17%, (b) 20%, (c) 22% and (d) 27%

propagation of the pit or by the appearance of short cracks at the bottom.

References

1. S. Fetni, Microstructure evolution and corrosion behaviour of an ASTM A213 T91 tube after long term creep exposure. *Eng. Failure Anal.* (2017). <https://doi.org/10.1016/j.engfailanal.2017.03.023>
2. A. Toumi, C. Boubahri, J. Briki et al., HSLA naval grade steel failure investigation in marine environment under ship hull operational conditions. *J Fail. Anal. Preven.* **21**, 2224–2233 (2021)
3. Grumbach, M. (2000). *Aciers microalliés*. Dans *Techniques de l'ingénieur Propriétés et usages des aciers et fontes*
4. Zghal, J. (2016). *Etude du comportement en fatigue à grand nombre de cycles d'un acier à haute limite d'élasticité HC360LA : endommagement, plasticité et phénomènes dissipatifs associés*. Paris
5. K. Berchem, M.G. Hocking, The influence of pre-straining on the corrosion fatigue performance of two hot-dip galvanised steels. *Corros. Sci.* **48**, 4094–4112 (2006)
6. T. Datta, Fractal behavior of surface oxide crack patterns on AISI 4140 high-strength low-alloy steel exposed to the simulated offshore environment. *Appl. Surf. Sci. Adv.* (2021). <https://doi.org/10.1016/j.apsadv.2021.100110>
7. T. Zhao, Corrosion fatigue crack initiation and initial propagation mechanism of E690 steel in simulated seawater. *Mater. Sci. Eng. A.* **708**, 181–192 (2017)
8. E.J. Dolley, B. Lee, The effect of pitting corrosion on fatigue life. *Fatigue Fract. Eng. Mater. Struct.* **23**, 555–560 (2000)
9. A.T. Kermanidis, P.V. Petroyiannis, Fatigue and damage tolerance behaviour of corroded 2024 T351 aircraft aluminum alloy. *Theor. Appl. Fract. Mech.* **43**, 121–132 (2005)
10. M. Talebi, M. Zeinoddini, Collapse of HSLA steel pipes under corrosion exposure and uniaxial inelastic cycling. *J. Constr. Steel Res.* **144**, 253–269 (2018)
11. H. Ma, J. Zhao, Comparative study on corrosion fatigue behaviour of high strength low alloy steel and simulated HAZ microstructures in a simulated marine atmosphere. *Int. J. Fatigue.* **137**, 105666 (2020)
12. S.T. Sivaprasad, Corrosion fatigue crack growth behaviour of naval steels. *Corros. Sci.* (2006). <https://doi.org/10.1016/j.corsci.2005.08.005>
13. COMSOL, *Multiphysics structural mechanics module users' guide*. (Burlington, USA, 2008)
14. Xu, L. (2013). *Assessment of corrosion defects on high-strength steel pipelines*. Calgary.
15. Y. Kondo, Prediction of fatigue crack initiation life based on pit growth. *Corrosion*. (1989). <https://doi.org/10.5006/1.3577891>

16. G.S. Chen, K.C. Wan, Transition from pitting to fatigue crack growth—modeling of corrosion fatigue crack nucleation in a 2024–T3 aluminum alloy. *Mater. Sci. Eng. A-Struct. Mater.* (1996). [https://doi.org/10.1016/S0921-5093\(96\)10414-7](https://doi.org/10.1016/S0921-5093(96)10414-7)
17. J. Lemaitre, Préviation de la progression des fissures de fatigue dans les structures minces renforcées. *Revue de Physique Appliquée, Société Française de Physique/EDP.* **9**(4), 667–672 (1974)

Publisher's Note Springer Nature remains neutral with regard to jurisdictional claims in published maps and institutional affiliations.

Springer Nature or its licensor (e.g. a society or other partner) holds exclusive rights to this article under a publishing agreement with the author(s) or other rightsholder(s); author self-archiving of the accepted manuscript version of this article is solely governed by the terms of such publishing agreement and applicable law.